iowa better concrete conference

Field Instrumentation for Load-Induced Fatigue Damage of Concrete Pavement Systems Under Superloads

Yongsung Koh(1), Halil Ceylan(2), Sunghwan Kim(3), and In Ho Cho(4)

(1) Department of Civil, Construction and Environmental Engineering, Iowa State University; Email: yskho27@iastate.edu

(2) Department of Civil, Construction and Environmental Engineering, Iowa State University; Email: hceylan@iastate.edu

(3) Department of Civil, Construction and Environmental Engineering, Iowa State University; Email: sunghwan@iastate.edu

(4) Department of Civil, Construction and Environmental Engineering, Iowa State University; Email: icho@iastate.edu

IOWA STATE UNIVERSITY

Acknowledgements

- Would like to express our sincere gratitude to including, but not limited to
  - Iowa Highway Research Board (IHRB) and Iowa Department of Transportation (DOT)
  - Iowa County Engineers Association (ICEA) Service Bureau, including Danny Waid, P.E. and Brian P. Moore, P.E.
  - Technical Advisory Committee (TAC) from Iowa County Engineers for **"TR 781, Development of Approaches to Quantify Superloads and Their Impacts on Iowa Road Infrastructure System"**
  - Many Research Team Members from ISU PROSPER and CCEE/InTrans/ISU

Background

What is the problem with the **superload**?

- High Gross Vehicle Weights (GVWs) or axle weights exceeding the United State's permit limit
- Non-standardized configurations of tires and axles representing a wide range of dimensions
- Slow moving behavior and wide vehicle width likely to exceed the lane-width of concrete pavements

→ **Unexpected fatigue damages on concrete pavement systems when subjected to superloads, including Implement of Husbandry (IoH) and Superheavy Loads (SHL), especially in the Midwestern region of the U.S.**

Objectives

(i) Computational determination of structural fatigue damages of Jointed Plain Concrete Pavements (JPCPs) when subjected to various types of superloads and the **(ii) field instrumentation**

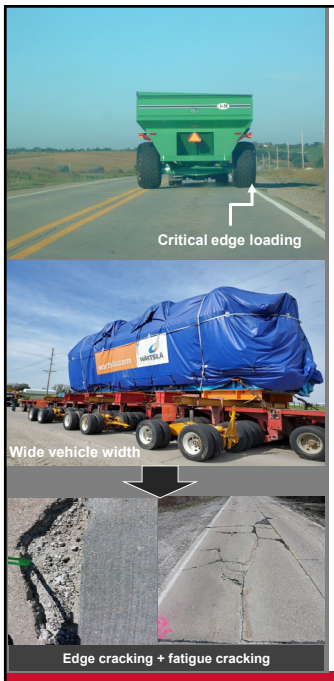

Background

What is the problem with the **superload**?

- High Gross Vehicle Weights (GVWs) or axle weights exceeding the United State's permit limit
- Non-standardized configurations of tires and axles representing a wide range of dimensions
- Slow moving behavior and wide vehicle width likely to exceed the lane-width of concrete pavements

→ **Unexpected fatigue damages on concrete pavement systems when subjected to superloads, including Implement of Husbandry (IoH) and Superheavy Loads (SHL), especially in the Midwestern region of the U.S.**

Objectives

(i) Computational determination of structural fatigue damages of Jointed Plain Concrete Pavements (JPCPs) when subjected to various types of superloads and the **(ii) field instrumentation**

Determination of Critical Loading Locations

FEM-based Mechanistic Analysis for Damage Ratio Calculation

Field Instrumentation and Monitoring

Remaining Tasks of Study: FEA Result Calibration Using the Field Data

Classification of Critical Loading Locations

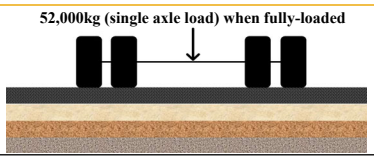

Type of IoHs	Grain cart	Manure tanker	Agricultural trailer	Agricultural truck
Number of IoHs	6	6	2	4
Gross Vehicle Weight (GVW) (kg)	35,000 ~ 85,000	42,000 ~ 76,000	20,000 ~ 44,000	24,000 ~ 35,000
Number of axle	1 ~ 3	2 ~ 4	2 ~ 3	2 ~ 3
Number of tire per axle	2 (single tier), 4 (dual tire)	2 (single tier)	2 (single tier)	2 (single tier)

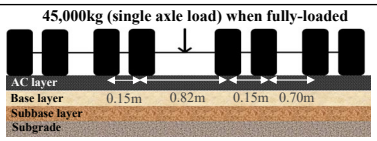

Type of SHLs	Single row modular type	Dual row modular type	Drop-deck type
Number of SHLs	8	5	3
Gross Vehicle Weight (GVW) (kg)	120,000 ~ 470,000	250,000 ~ 960,000	80,000 ~ 145,000
Number of axle	8+	8+	13 ~ 19
Number of tire per axle	4 (single tier), 8 (dual tire)	8 (single tier), 16 (dual tire)	4 ~ 8 (dual tire)

Determination of Critical Loading Locations

FEM-based Mechanistic Analysis for Damage Ratio Calculation

Field Instrumentation and Monitoring

Remaining Tasks of Study: FEA Result Calibration Using the Field Data

Classification of Critical Loading Locations

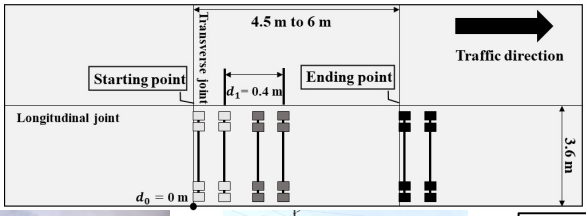

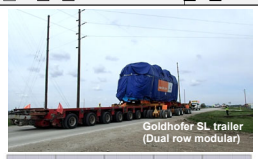

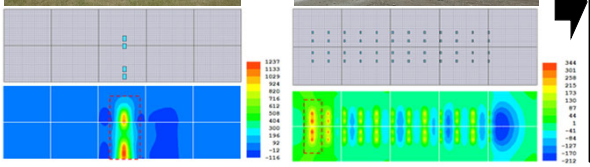

Classification of superloads

7 classes for IoHs classified by different axle types

4 classes for SHLs classified by different trailer types

Note: Details of superload classification can be found in Koh et al. 2022

Determination of Critical Loading Locations

FEM-based Mechanistic Analysis for Damage Ratio Calculation

Field Instrumentation and Monitoring

Remaining Tasks of Study: FEA Result Calibration Using the Field Data

Classification of Critical Loading Locations

Classification of IoHs according to the critical loading locations

Case	Category	Type	Critical loading location	Relevant IoHs
Critical tensile stresses at the bottom of PCC slab	1	**IoH with single-axle**	Single-axle located near the mid-slab	Kinze 1305 flotation, Kinze 1305 row crop, Kinze 1051, J&M 1151
	2	**IoH with tandem-axle**	(2-1) For small axle spacing (< 86 in): tandem-axle located symmetrically within a PCC slab; (2-2) For high axle spacing (> 130 in): one of all axles locates near the mid-slab	(2-1) Balzer 1725, Balzer 6800 magnum, GEA EL48-4D (2-2) J&M 555 wagon, J&M 755 wagon
	3	**IoH with tridem-axle**	**[In case of JPCP with transverse joint: 15 ft, LTE: 50%]** (3-1) For small axle spacing (< 75 in): two of all axles located symmetrically within a PCC slab; (3-2) For high axle spacing (> 78 in): one outer axle located on another slab away from the joint **[In case of JPCP with transverse joint: 15 ft and 17 ft, LTE: 90%]** (3-3) Two of all axles located symmetrically within a PCC slab **[In case of JPCP with transverse joint: 20 ft, LTE: 90%]** (3-4) All three axles are located symmetrically within a PCC slab	(3-1) GEA EL48-6D (3-2) Balzer 2550, Balzer 9500 magnum (3-3) and (3-4) GEA EL48-6D, Balzer 2550, Balzer 9500 magnum
	4	**IoH with quad-axle**	**[In case of JPCP with transverse joint: 15 ft and 17 ft, LTE: 50% and 90%]** (4-1) Two of all axles located symmetrically within a PCC slab **[In case of JPCP with transverse joint: 20 ft, LTE: 90%]** (4-2) Three of all axles located symmetrically within a PCC slab	(4-1) and (4-2) GEA EL48-8D, NUHN QT Quad Tanks
	5	**IoH with a special type of axle configuration**	Front axle located near the mid-slab	Terragator 2550, Terragator TG7300C, Terragator TG8400C, Case 340B
Critical tensile stresses at the top of PCC slab	1	**IoH with single, tandem, tridem, or quad-axle**	One outer axle located upon or near the transverse joint	Kinze 1305 flotation, Kinze 1305 row crop, Kinze 1051, J&M 1151, Balzer 1725, Balzer 6800 magnum, GEA EL48-4D, J&M 555 wagon, J&M 755 wagon, GEA EL48-6D, Balzer 2550, Balzer 9500 magnum, GEA EL48-8D, NUHN QT Quad Tanks
	2	**IoH with a special type of axle configuration**	One axle with the highest axle weight located upon or near the transverse joint	Terragator 2550, TerragatorTG 7300, Terragator TG8400C, Case 340B

Note: Details of superload classification can be found in Koh et al. 2022

Determination of Critical Loading Locations

FEM-based Mechanistic Analysis for Damage Ratio Calculation

Field Instrumentation and Monitoring

Remaining Tasks of Study: FEA Result Calibration Using the Field Data

Classification of Critical Loading Locations

Classification of SHLs according to the critical loading locations

Case	Category	Type	Critical loading location	Relevant SHLs
Critical tensile stresses at the bottom of PCC slab	1	**SHL with modular type trailers**	**[In case of JPCP with transverse joint: 15 ft, LTE: 50% and 90%]** (1-1) The front or rear axle is located near the mid-slab, and only two axles, including the front or rear axle with the next axle, exist in a slab **[In case of JPCP with transverse joint: 17 ft, LTE: 90%]** (1-2) The first or last three axles are symmetrically located within a slab **[In case of JPCP with transverse joint: 20 ft, LTE: 90%]** (1-3) The first or last four axles are symmetrically located within a slab	(1-1), (1-2), and (1-3) All the modular types of SHL
	2	**SHL with drop-deck type trailers**	Drop-deck type trailer with tandem-axle groups or tridem-axle groups located with the highest axle weight group in the same way as IoHs with a tandem-axle (2-1) or a tridem-axle (3-1) having small axle spacing	All the drop-deck types of SHL
Critical tensile stresses at the top of PCCslab	1	**SHL with modular type trailers**	One outer axle located upon or near the transverse joint	All the modular types of SHL
	2	**SHL with drop-deck type trailers**	Drop-deck type trailer with tandem and tridem-axle groups located as two separate axle groups near transverse joints having one non-loaded PCC slab between them	All the drop-deck types of SHL

Note: Details of superload classification can be found in Koh et al. 2022

Determination of Critical Loading Locations

FEM-based Mechanistic Analysis for Damage Ratio Calculation

Field Instrumentation and Monitoring

Remaining Tasks of Study: FEA Result Calibration Using the Field Data

Mechanistic-based Damage Ratio Calculation

Finite Element Method (FEM)-based JPCP analysis (software: ISLAB2005)								
Local road					Highway			
Thickness of PCC layer (mm)					Thickness of PCC layer (mm)			
180, 230					250, 330			
Composite modulus of subgrade reaction (MPa/m)					Composite modulus of subgrade reaction (MPa/m)			
Season	Spring	Summer	Fall	Winter	Spring	Summer	Fall	Winter
	14	33	33	68	14	33	33	68
Transverse joint spacing (m): 4.5					Transverse joint spacing (m): 5.2, 6.0			
Elastic modulus of PCC layer (MPa): 27600					Elastic modulus of PCC layer (MPa): 27600			
Traffic loadings					Traffic loadings			
IoH: 18 types × 4 payload levels = 72 types					IoH: 18 types × 4 payload levels = 72 types			
SHL: 16 types × 4 payload levels = 64 types					SHL: 16 types × 4 payload levels = 64 types			
FHWA class 9 truck (reference) = 1 type					FHWA class 9 truck (reference) = 1 type			
Total analysis cases: 10,960 cases					Total analysis cases: 21,920 cases			

S-N curve from previous experimental tests by ISU

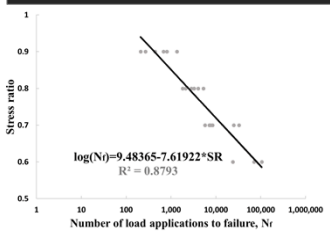

Damage ratio for bottom-up transverse cracking

Damage ratio for bottom-up transverse cracking =

$$\frac{\frac{1}{N_{f,b,superload}}}{\frac{1}{N_{f,b,class\ 9}}} = \frac{N_{f,b,class\ 9}}{N_{f,b,superload}} \text{ applying Miner's rule}$$

Damage ratio for top-down transverse cracking

Damage ratio for top-down transverse cracking =

$$\frac{\frac{1}{N_{f,t,superload}}}{\frac{1}{N_{f,t,class\ 9}}} = \frac{N_{f,t,class\ 9}}{N_{f,t,superload}} \text{ applying Miner's rule}$$

Note: ISU experimental results for fatigue testing of PCC slabs from Klaiber et al. 1979

Determination of Critical Loading Locations

FEM-based Mechanistic Analysis for Damage Ratio Calculation

Field Instrumentation and Monitoring

Remaining Tasks of Study: FEA Result Calibration Using the Field Data

Mechanistic-based Damage Ratio Calculation

Damage ratio for bottom-up transverse cracking of IoHs (left) and SHLs (right)

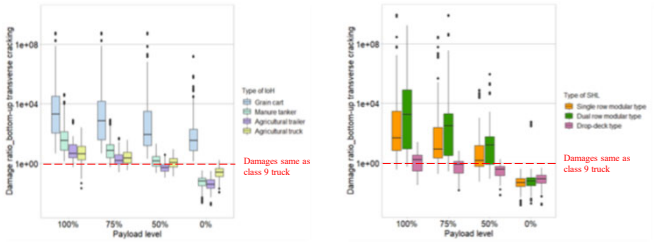

Damage ratio for top-down transverse cracking of IoHs (left) and SHLs (right)

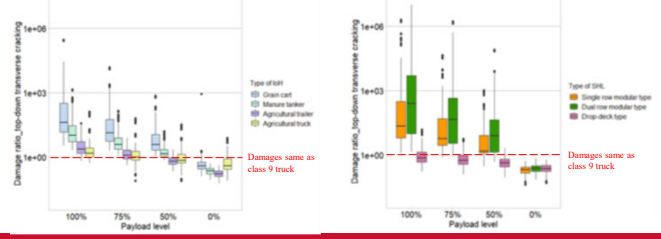

Determination of Critical Loading Locations

FEM-based Mechanistic Analysis for Damage Ratio Calculation

Field Instrumentation and Monitoring

Remaining Tasks of Study: FEA Result Calibration Using the Field Data

Field Instrumentation - Data Acquisition System

Field instrumentation site – K45 road (full-depth PCC pavement reconstruction)

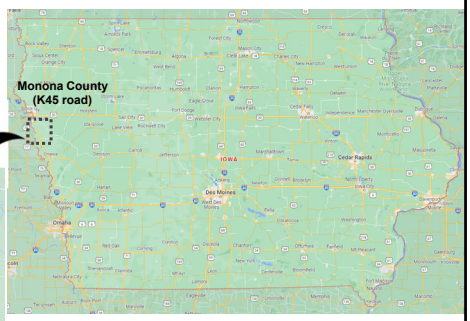

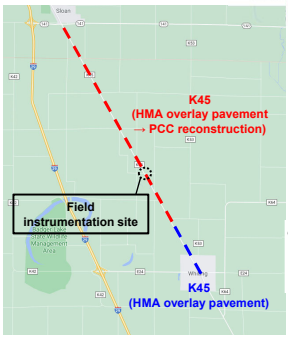

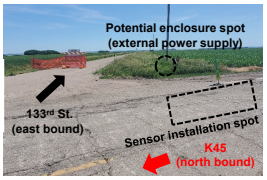

Determination of Critical Loading Locations

FEM-based Mechanistic Analysis for Damage Ratio Calculation

Field Instrumentation and Monitoring

Remaining Tasks of Study: FEA Result Calibration Using the Field Data

Field Instrumentation - Data Acquisition System

Field instrumentation site – K45 road (full-depth PCC pavement reconstruction)

Excavation of existing pavement

Removal

JPCP construction

Gradation

Determination of Critical Loading Locations

FEM-based Mechanistic Analysis for Damage Ratio Calculation

Field Instrumentation and Monitoring

Remaining Tasks of Study: FEA Result Calibration Using the Field Data

Field Instrumentation - Data Acquisition System

Pre-instrumentation activities

LWD test

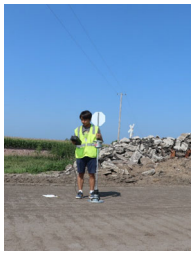

DCP test

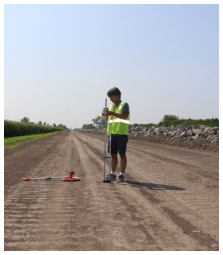

Sand cone test

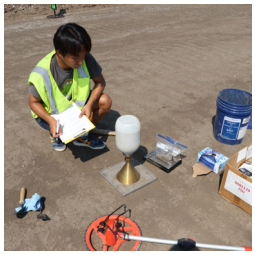

Drilling the holes to install the sensor trees

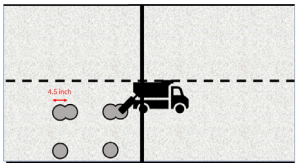

Determination of Critical Loading Locations

FEM-based Mechanistic Analysis for Damage Ratio Calculation

Field Instrumentation and Monitoring

Remaining Tasks of Study: FEA Result Calibration Using the Field Data

Field Instrumentation - Data Acquisition System

Pre-instrumentation activities

Conceptual configuration of data acquisition system

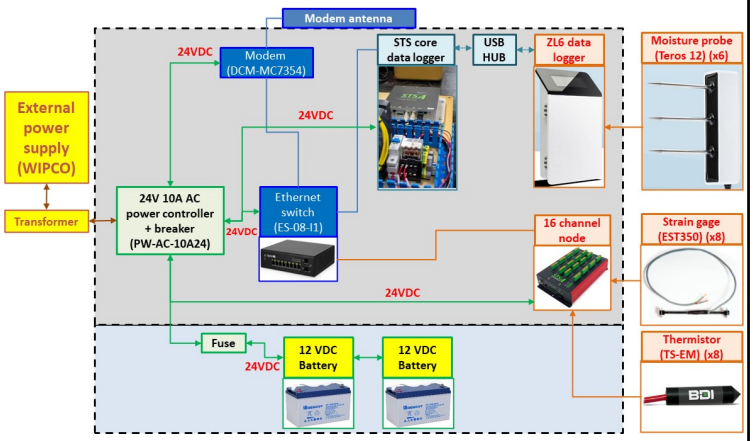

Determination of Critical Loading Locations

FEM-based Mechanistic Analysis for Damage Ratio Calculation

Field Instrumentation and Monitoring

Remaining Tasks of Study: FEA Result Calibration Using the Field Data

Field Instrumentation - Data Acquisition System

Pre-instrumentation activities

Cross section view

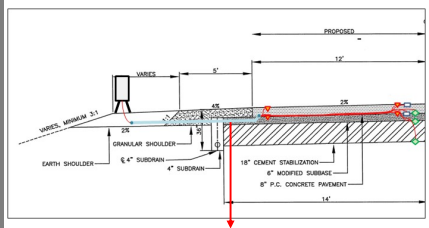

Plane view

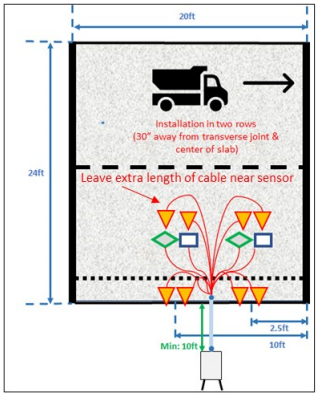

Flexible PVC pipe protecting sensor cables

Determination of Critical Loading Locations

FEM-based Mechanistic Analysis for Damage Ratio Calculation

Field Instrumentation and Monitoring

Remaining Tasks of Study: FEA Result Calibration Using the Field Data

Field Instrumentation - Data Acquisition System

Pre-instrumentation activities

Pre-testing in laboratory

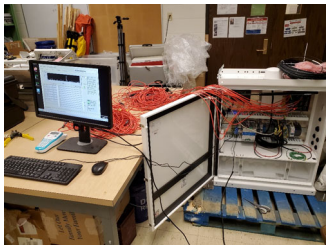

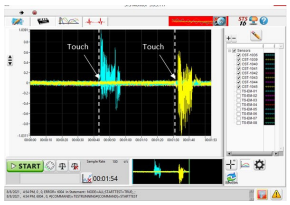

Wooden supports for fixing the enclosure

Determination of Critical Loading Locations

FEM-based Mechanistic Analysis for Damage Ratio Calculation

Field Instrumentation and Monitoring

Remaining Tasks of Study: FEA Result Calibration Using the Field Data

Field Instrumentation - Data Acquisition System

Sensor installation and cable protection

Determination of Critical Loading Locations

FEM-based Mechanistic Analysis for Damage Ratio Calculation

Field Instrumentation and Monitoring

Remaining Tasks of Study: FEA Result Calibration Using the Field Data

Field Instrumentation - Data Acquisition System

Concrete paving and sensor protection

Determination of Critical Loading Locations

FEM-based Mechanistic Analysis for Damage Ratio Calculation

Field Instrumentation and Monitoring

Remaining Tasks of Study: FEA Result Calibration Using the Field Data

Field Instrumentation - Data Acquisition System

Post-instrumentation activities

External power supply for data acquisition system

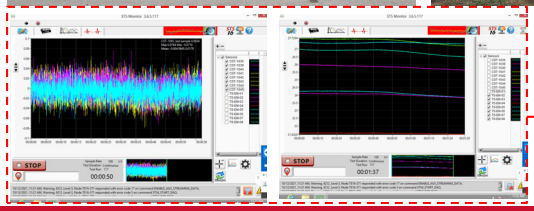

Collecting pavement responses remotely for a long-term period

Determination of Critical Loading Locations

FEM-based Mechanistic Analysis for Damage Ratio Calculation

Field Instrumentation and Monitoring

Remaining Tasks of Study: FEA Result Calibration Using the Field Data

Field Instrumentation - Data Acquisition System

Field data analysis

Strain data of PCC slab (12/19/2021)

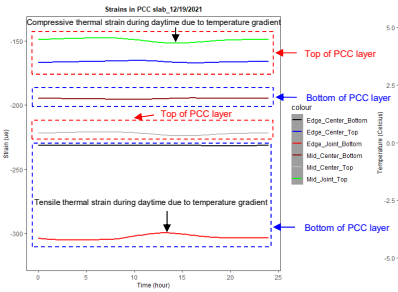

Temperatue data of PCC slab (12/19/2021)

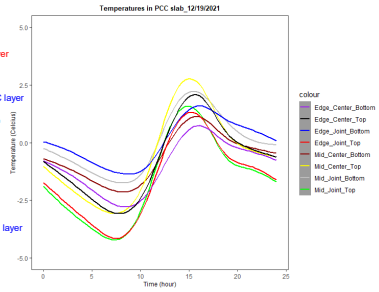

- Compressive thermal strains are induced at the top of the PCC slab and tensile thermal strains at the bottom of the PCC slab during the daytime due to temperature gradients
- Tensile thermal strains are induced at the top of the PCC slab and compressive thermal strains at the bottom of the PCC slab during the nighttime due to temperature gradients

Determination of Critical Loading Locations

FEM-based Mechanistic Analysis for Damage Ratio Calculation

Field Instrumentation and Monitoring

Remaining Tasks of Study: FEA Result Calibration Using the Field Data

Field Instrumentation - Data Acquisition System

Field data analysis

Tensile strain at the bottom of the PCC slab when subjected to traffic loadings

Compressive strain at the top of the PCC slab when subjected to traffic loadings

Strain data of PCC slab (6-axles traffic)

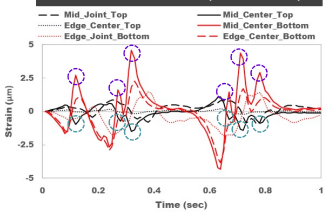

Strain data of PCC slab (4-axles traffic)

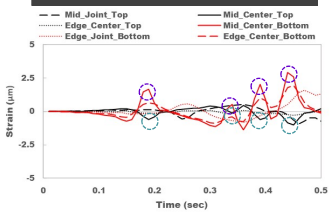

Strain data of PCC slab (3-axles traffic)

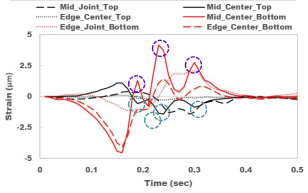

Strain data of PCC slab (2-axles traffic)

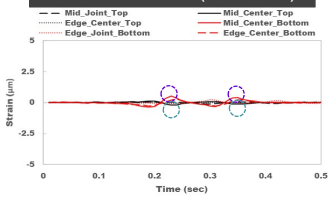

Determination of Critical Loading Locations

FEM-based Mechanistic Analysis for Damage Ratio Calculation

Field Instrumentation and Monitoring

Remaining Tasks of Study: FEA Result Calibration Using the Field Data

Remaining Tasks – FEA Result Calibration

Field data analysis

Portable Weight-in-Motion (P-WIM) system

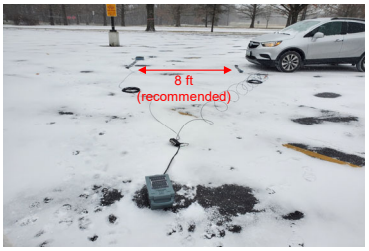

Number	Year	Month	Day	Hour	Minute	Second	Lane	Class	Speed	Num Axle	GVW	Wheelbs	Wt1	Spc1	Wt2	Spc2	Wt3	Spc3	Wt4	Spc4	Wt5	Spc5
1	2	1	1	15	12	23	1	4	10	2	18200	17.8	9100	17.8	9100							
2	2	1	1	15	20	1	1	4	10	2	18290	17.9	9150	17.9	9140							
3	2	1	1	15	31	41	1	4	10	2	18270	18.3	8890	18.3	9380							

GVW

1st axle weight

2nd axle weight

Determination of Critical Loading Locations

FEM-based Mechanistic Analysis for Damage Ratio Calculation

Field Instrumentation and Monitoring

Remaining Tasks of Study: FEA Result Calibration Using the Field Data

Remaining Tasks – FEA Result Calibration

Field data analysis

Field strain data (6-axles traffic)

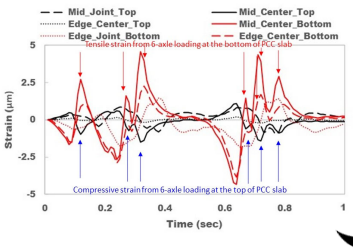

FEA strain results (6-axles traffic with 20% payload level)

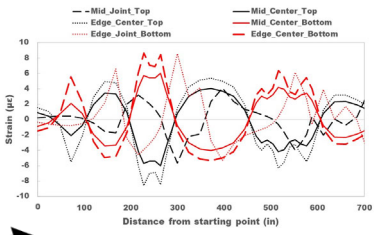

FEA result calibration using field data

- **FEA strain results need to be calibrated using field strain data from the data acquisition system + P-WIM system installed in the field**

Summary and Discussions

- A total of 34 types of superload can be classified into **seven categories of IoHs** and **four categories of SHLs**, depending on their **critical loading locations**
- **Grain cart type IoHs** and **dual-row modular type SHLs** show much higher damage ratios regarding the bottom-up and top-down transverse cracking of JPCPs
- Decreasing the payload levels of all the superload types from 100% to 50% significantly reduced the fatigue cracking damage ratios reaching to one
- Field instrumentation was conducted at **K45 road in Monona county** to monitor and evaluate the fatigue damages of JPCP when subjected to the superload traffic
- **Concrete strain gauges and thermistors** on the top and bottom of the PCC layer at various critical pavement response positions were installed in the field and connected to the data loggers having consistent external power supply
- **Long-term field data monitoring** is being performed to evaluate the fatigue damages according to different types of traffic with various payload levels
- The FEA results will be calibrated shortly using the field data from the data acquisition system and P-WIM system installed in the field

Author Information

Yongsung Koh

Ph.D. student

Research Assistant

yskho27@iastate.edu

Dr. Halil Ceylan, Dist.M.ASCE

Pitt-Des Moines, Inc. Professor in CCEE

Director, Program for Sustainable Pavement Engineering and Research (PROSPER)

hceylan@iastate.edu

Dr. Sunghwan Kim, P.E.

Associate Director of PROSPER

sunghwan@iastate.edu

Dr. In Ho Cho

Associate Professor of CCEE department in Iowa State University

icho@iastate.edu